Available online at www.sciencedirect.com

ScienceDirect

Nuclear and Particle Physics Proceedings 273–275 (2016) 162–169

www.elsevier.com/locate/nppp

The status of the construction of MICE Step IV ☆

K. Long[1]

Department of Physics, Imperial College London, Exhibition Road, London SW7 2AZ, UK.

Abstract

Muon beams of low emittance provide the basis for the intense, well-characterised neutrino beams necessary to elucidate the physics of flavour at the Neutrino Factory and to provide lepton-anti-lepton collisions at energies of up to several TeV at the Muon Collider. The International Muon Ionization Cooling Experiment (MICE) will demonstrate ionization cooling; the technique by which it is proposed to reduce the phase-space volume occupied by the muon beam at such facilities. In an ionization-cooling channel, the muon beam is caused to pass through a material (the absorber) in which it looses energy, the energy lost is then replaced using RF cavities. The combined effect of energy loss and re-acceleration is to reduce the transverse emittance of the beam (transverse cooling).

MICE is being constructed in a series of Steps. At Step IV, MICE will be able to study the properties of liquid hydrogen and lithium hydride that affect cooling. A solenoidal spectrometer will measure emittance upstream and downstream of the absorber vessel. The muon beam will be focused at the absorber by a focusing coil. The construction of Step IV at the Rutherford Appleton Laboratory is well advanced and is scheduled to be complete early in 2015. The status of the construction project will be described together with the performance of the principal components. Once the Step IV programme has been completed, the apparatus will be reconfigured to allow the MICE collaboration to demonstrate ionization cooling. This will require two single-cavity modules to be inserted one upstream and one downstream of a central absorber. The status of the preparations for the MICE demonstration of ionization cooling will also be described briefly.

Keywords: Neutrino oscillations, Neutrino Factory, Muon Collider

1. Introduction

Stored muon beams have been proposed as the source of neutrinos at the Neutrino Factory [1, 2, 3, 4, 5, 6, 7, 8] and as the means to deliver multi-TeV lepton-antilepton collisions at the Muon Collider [9, 10]. In such facilities the muon beam is produced from the decay of pions produced in the bombardment of a target by a high-power proton beam. The tertiary muon beam is captured in a solenoidal channel and occupies a large volume in phase space. To optimise the muon yield while maintaining a suitably small aperture in the muon-acceleration systems requires that the muon-beam phase space be reduced (cooled) prior to acceleration. The short muon lifetime makes traditional cooling techniques unacceptably inefficient when applied to muon beams. Ionization cooling, in which the muon beam is passed through material (the absorber) and subsequently accelerated, is the technique by which it is proposed to cool the beam. Passing through the absorber, the muon beam looses longitudinal and transverse momentum in equal proportion. The re-acceleration restores only the longitudinal component. A reduction in the transverse phase-space volume occupied by the beam is therefore achieved by the energy-loss–re-acceleration cycle. The net cooling effect required by the Neutrino Factory or Muon Col-

☆ Talk presented at the 37th International Conference on High Energy Physics, Valencia, 2nd to 9th July 2014.

Email address: K.Long@Imperial.Ac.UK (K. Long)

[1] On behalf of the MICE collaboration.

http://dx.doi.org/10.1016/j.nuclphysbps.2015.09.020

2405-6014/© 2016 Published by Elsevier B.V.
This is an open access article under the CC BY license (http://creativecommons.org/licenses/by/4.0/).

Table 1: Comparison of the cooling performance of a variety of possible absorber materials. The figure of merit ($\mathcal{F}$) is defined in the text. The relative transverse cooling performance is obtained by dividing the figure of merit for a particular material by that of liquid hydrogen. The material parameters used to evaluate $\mathcal{F}$ have been taken from [12].

Material	$\mathcal{F}$	**Relative transverse cooling performance**
Liquid hydrogen	258	1
Liquid helium	183	0.5
Lithium hydride	151	0.34
Carbon	74	0.08

lider is achieved by the repeated application of the cooling cycle.

If it is assumed that the divergence of the muon beam is not too large (the paraxial approximation) and that the magnetic field is sufficiently uniform then the evolution of the normalised transverse emittance, $\epsilon_\perp^{\mathrm{n}}$, with distance, x, along the beam may be approximated by [11]:

$$\frac{d\epsilon_\perp^{\mathrm{n}}}{dx} \approx -\frac{\epsilon_\perp^{\mathrm{n}}}{\beta^2 E}\left\langle\frac{dE}{dx}\right\rangle + \frac{\beta_\perp (0.014\,\mathrm{GeV})^2}{2\beta^3 E m_\mu X_0}\,; \qquad (1)$$

where E is the beam energy, β the relativistic velocity of the muon, $\beta_\perp$ is the transverse betatron function and m_μ is the muon mass. Cooling is generated from the energy-loss term which is proportional to the specific ionization, dE/dx, of the absorber material. Multiple Coulomb scattering causes heating, the size of the heating effect being inversely proportional to the radiation length, X_0. The net cooling effect is determined by the balance between the change in emittance generated by the energy-loss term and the heating term and optimum cooling performance will be obtained using a material of low atomic number so that both dE/dx and X_0 are large. Taking:

$$\mathcal{F} = X_0 \times \frac{dE}{dX}\,; \qquad (2)$$

to define a figure of merit, $\mathcal{F}$, the cooling efficacy of different materials can be assessed. Table 1 compares the figure of merit for a variety of possible absorber materials. Practical designs for cooling channels have been developed using liquid hydrogen (LH_2) and/or lithium hydride (LiH). Therefore, the MICE programme includes the evaluation of the cooling performance of LH_2 and LiH as well as a systematic study of the effect the optics of the cooling cell has on its performance.

This contribution is organised as follows. An overview of the MICE programme will be given in section 2. A summary of the status of the Step IV construction project is given in section 3 and the status of preparations for the MICE demonstration of ionization cooling is summarised in section 4. Finally, conclusions are drawn in section 5.

2. Overview

The MICE collaboration was approved to design, build, commission and operate a section of a realistic cooling channel and to measure its performance using a number of absorber materials, in a variety of modes of operation and under a range of beam conditions [13, 14]. The experiment is being constructed in three stages. In the first stage (referred to as Step I), the MICE Muon Beam (MMB) on ISIS was constructed together with the instrumentation necessary to characterise the beam [15]. Step I is now complete and the MMB has been shown to deliver the performance necessary to deliver the MICE physics programme [16].

The second stage of the experiment (referred to as Step IV) is shown schematically in figure 1. The absorber module is placed inside a superconducting "focus-coil" (FC) module. Focusing the beam at the absorber provides a small value of $\beta_\perp$, thereby increasing the net cooling effect (see equation 1). A solenoidal tracking spectrometer is placed upstream of the absorber/focus-coil (AFC) module to measure the muon-beam phase space before it passes through the absorber. A second spectrometer module is placed downstream of the AFC to measure the muon-beam phase space as the beam emerges from the absorber. The spectrometers have been designed such that the change in the properties of the beam as it passes through the absorber (for example $\epsilon_\perp^{\mathrm{n}}$) can be measured with a relative precision at the per-cent level [17]. Upstream of the first spectrometer, time-of-flight (ToF) hodoscopes and Cherenkov (CKOV) counters will be used to reject the small residual pion contamination in the beam [16]. The ToF system will also be used to trigger the experiment and, combined with the upstream spectrometer, measure the longitudinal phase-space of the incoming beam. Downstream of the experiment, a ToF hodoscope, a lead-scintillator calorimeter (the KL) and a totally active scintillator calorimeter (the Electron Muon Ranger, EMR) will reject electrons (positrons) from muon decay and determine the longitudinal phase-space of the beam as it emerges from the absorber [18, 19]. Both LH_2 and LiH absorbers will be used at Step IV [20, 21]. Commissioning is scheduled to start in the late spring of

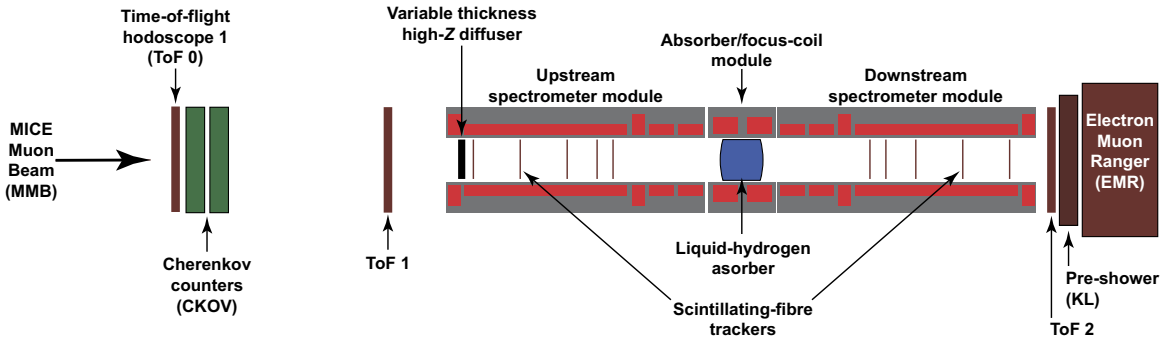


Figure 1: Schematic diagram of the Step IV configuration of MICE. The muon beam enters from the left of the figure. The beam-line instrumentation (the time-of-flight, ToF, hodoscopes, the Cherenkov (CKOV) counters, the pre-shower, KL, detector and the Electron Muon Ranger, EMR) are indicated. The spectrometer solenoids, and the scintillating-fibre trackers they contain are shown upstream and downstream of the central absorber/focus-coil (AFC) module.

2015 and data taking in the Step IV configuration will continue until the summer of 2016.

The MICE demonstration of ionization cooling will be performed by adding two, 201 MHz, cavity modules one upstream and another downstream of the AFC module as shown in figure 2. The principal absorber will be LiH. Secondary absorbers will be placed between the cavities and the spectrometers to increase the cooling effect and to protect the sensitive scintillating-fibre trackers from X-rays and dark current electrons produced in the cavities. The reconfiguration of the Step IV experiment to include the two single-cavity modules will start at the end of Step IV data taking. The schedule shows that commissioning of the equipment necessary to demonstrate ionization cooling will start in late spring 2017.

The MICE physics programme is summarised in table 2. At Step IV, the material properties of LH_2 and LiH will be measured and the change in $\epsilon_\perp^n$ as a function of the optics of the magnetic channel will be studied. The addition of the two single cavity modules will allow ionization cooling, i.e. the reduction of the transverse emittance $\epsilon_\perp$ to be measured (where $\epsilon_\perp = p_\mu \epsilon_\perp^n$ and p_μ is the muon momentum). In this configuration it will also be possible to study the way in which the longitudinal phase space (for example the longitudinal emittance, $\epsilon_\parallel$) and the canonical angular momentum, $\mathcal{L}$, vary as the beam is cooled.

Table 2: MICE physics programme

Step IV:
Material properties of LH_2 and LiH
Observation of $\epsilon_\perp^n$ reduction
MICE demonstration of ionization cooling:
Observation of $\epsilon_\perp$ reduction with re-acceleration
Observation of $\epsilon_\perp$ reduction and $\epsilon_\parallel$ evolution
Observation of $\epsilon_\perp$ reduction and $\epsilon_\parallel$ and angular momentum evolution[†]

[†] Requires systematic study of "flip" optics.

3. Status of Step IV

Figure 3 shows the status of the implementation of Step IV in the MICE Hall at the Rutherford Appleton Laboratory (RAL). The spectrometer solenoids, each fitted with scintillating-fibre tracker, have been installed on the beamline. The AFC module has also been installed. The two bellows that link the focus coil with the neighbouring spectrometer module have been fitted. The LH_2-delivery system, which has been commissioned into a test cryostat, may be seen on the mezzanine behind the down-stream spectrometer solenoid. The EMR, KL and ToF detectors may also be seen in the figure. The cryogenic, electrical, vacuum and water systems that are required to serve the experiment are not shown but are at an advanced stage of preparation. More details on the principal components of Step IV are given in the paragraphs that follow.

3.1. The tracker modules

Each tracker module is composed of a scintillating-fibre tracking detector installed within a spectrometer solenoid.

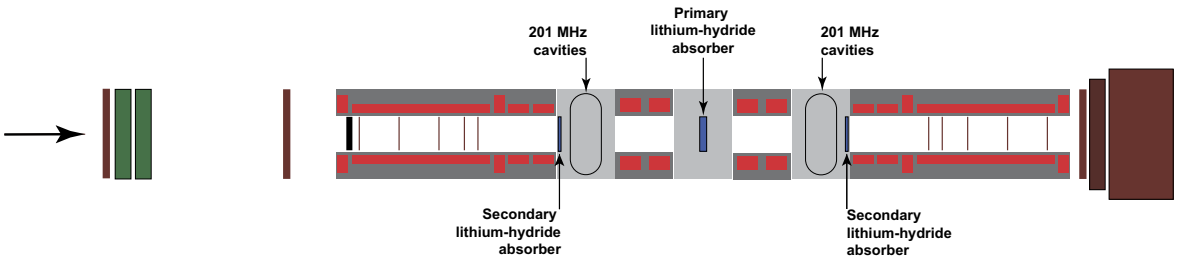


Figure 2: Schematic diagram of the configuration that will be used for the MICE demonstration of ionization cooling. Two single 201 MHz cavity modules and a focus-coil module are added to the Step IV configuration. The central lithium-hydride absorberis sandwiched between the focus-coil and single-cavity modules. Two secondary lithium-hydride absorbers placed between the cavities and the spectrometer modules increase the cooling effect and protect the trackers from x-rays and dark-current electrons.

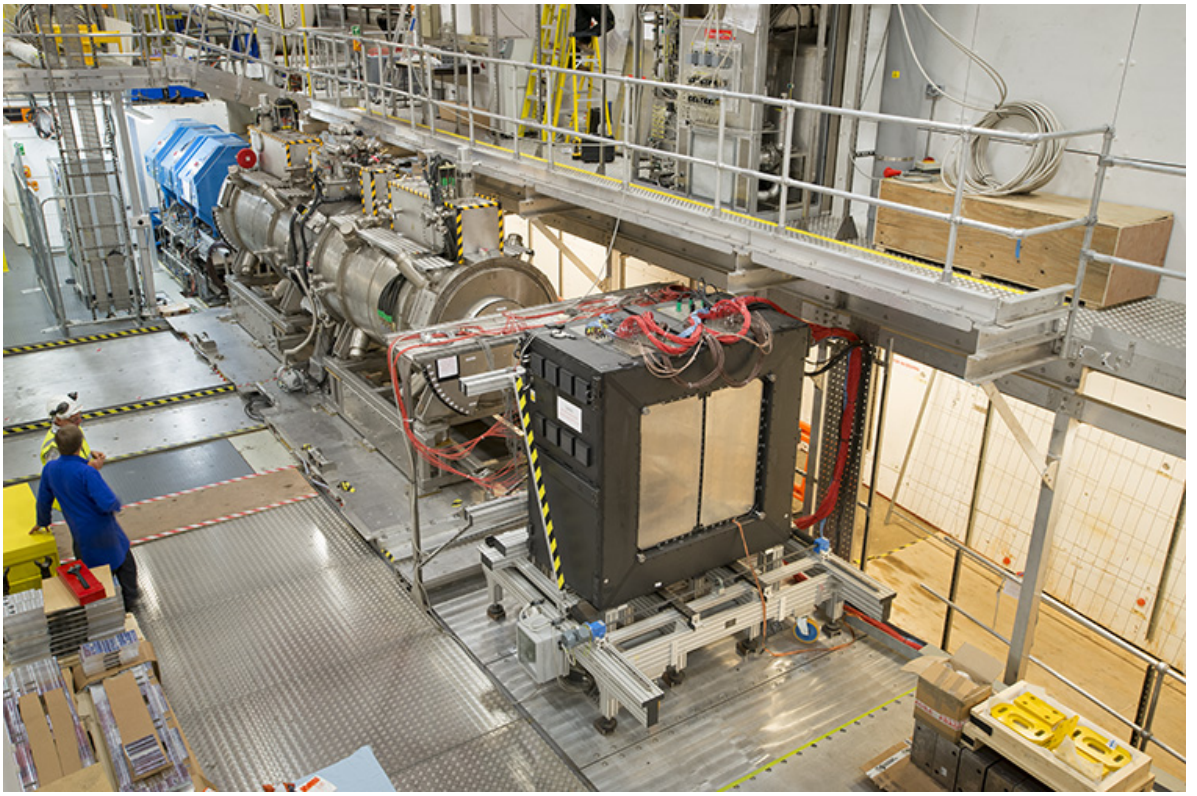


Figure 3: Photograph of the state of construction of MICE Step IV taken in August 2014. In the background, the final quadrupole triplet that focuses the beam into MICE may be seen (blue). The upstream spectrometer, the absorber/focus-coil module and the downstream spectrometer may then be seen in front of the downstream instrumentation (ToF2, KL and EMR). The liquid-hydrogen delivery system may be seen on the mezzanine above the EMR.

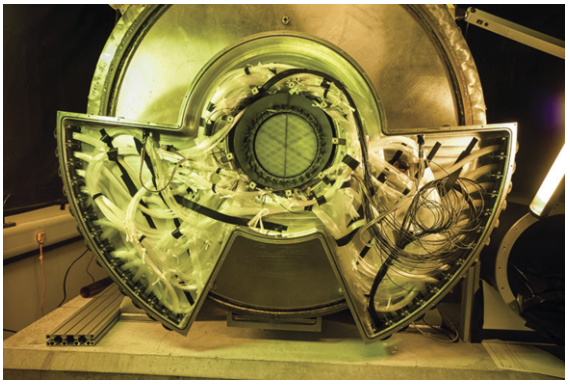


Figure 4: End view of the upstream tracker showing the routing of the clear-fibre light-guides. The upstream surface of the most upstream of the tracker stations can be seen in the centre of the bore of the spectrometer solenoid.

Each spectrometer solenoid (SS) is composed of five superconducting coils wound on a single bobbin. A "central" coil 120 cm long and surrounded by short "end coils" provides a field of 4 T, uniform at the percent level over the tracking volume. Two "match" coils follow and are used to match the beam from from the spectrometer into the focus-coil module. Both SSs were successfully trained to 102% of the maximum operating current. Measurements of the magnetic field produced by the magnet have been made and are being parameterised for use in the reconstruction and simulation software.

Charged-particle tracking is performed using a tracker composed of five planar scintillating-fibre stations. Each station is composed of three doublet-layers of scintillating fibres laid out in a 'u, v, w' arrangement. To reduce multiple Coulomb scattering of muons to an acceptable level, a fibre diameter of 350 μm was used. Seven scintillating fibres are ganged for readout through a single 1.05 mm clear-fibre light-guide. Figure 4 shows the completion of the routing of the clear-fibre waveguides of the upstream tracker. The scintillation light is detected using Visible Light Photon Counters (VLPCs) [22, 23] and read out using the DØ Central Fiber Tracker (CFT) optical readout and electronics system [24, 25].

3.2. Absorber/focus-coil module

The focus-coil (FC) modules each consist of two coils wound on a single bobbin. The coils can be run with the same polarity ("solenoid mode") or with opposite polarities ("flip mode"). The first module (FC1) trained rapidly to full current (110 A) in solenoid mode. In flip mode, training ceased at 188 A after $\sim$ 15 quenches.



Figure 5: The liquid-hydrogen absorber vessel prior to installation in the focus-coil module.

FC1 is stable in operation at 180 A, a current $\sim$ 5% below that required to produce the nominal beta at teh absorber of 42 cm at a momentum of 200 MeV/c. The training of the second module FC2 was more satisfactory as it reached the specified maximum currents in solenoid (110 A) and flip (225 A) modes essentially without training.

The magnetic field of FC1 and FC2 have each been measured in both flip and solenoid modes. In the Step IV configuration, the experiment will run using FC2. The FC currents required in the configuration to be implemented for MICE to demonstrate ionization cooling (figure 2) are lower than the FC currents required at Step IV. The completion of the MICE programme may therefore proceed using the two FC modules that have been commissioned at RAL.

The liquid-hydrogen absorber that will be used at Step IV is shown in figure 5. The vessel has a volume of 20.71 and is closed by aluminium windows shaped so as to minimise the length of aluminium traversed by the beam. On axis, where the LH_2 volume has a length of 35 cm, the windows are each 120 μm thick. The absorber was built and tested at KEK and has been delivered to RAL where it has been installed in the focus coil. The lithium-hydride absorber, shown in figure 6, is a 65 mm thick disk. Both the disk and the support structure have been fabricated in the US.

3.3. Partial Return Yoke

A soft iron partial return yoke (PRY) is required to provide a flux return and to protect equipment in the

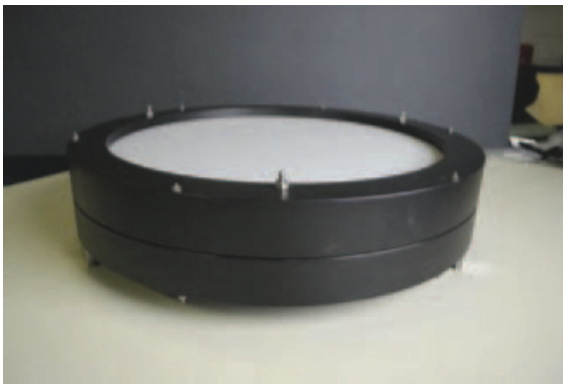


Figure 6: The lithium-hydride absorber.

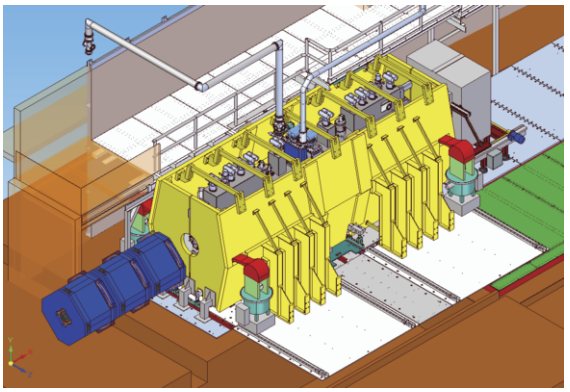


Figure 7: Schematic drawing of the partial return yoke surrounding the Step IV configuration of MICE.

MICE Hall from the magnetic flux created by the superconducting solenoids that provide the MICE magnetic lattice. A schematic drawing of the PRY is shown in figure 7. The procurement of all components of the PRY is well advanced and the installation of the floor fixings is underway at RAL.

4. Demonstration of ionization cooling

The MICE demonstration of ionization cooling will be carried out using the configuration sketched in figure 2. To implement this configuration, two single cavity modules are required in addition to the equipment that has already been constructed, commissioned and delivered to the Rutherford Appleton Laboratory. Figure 8 shows the first single-cavity fully dressed inside its vacuum vessel (the "Single Cavity Test Stand", SCTS). The cavity body is constructed from oxygen-free high-conductivity copper. The cavity is tuned by deformation using the six tuner assemblies that can be seen in the figure. The cavity has been installed in the Muon Test Area (MTA) at Fermilab for commissioning and testing. Initial results are encouraging; in the absence of magnetic field the cavity was powered to a gradient of 8 MV/m, the nominal accelerating gradient in MICE, without producing a measurable flux of X-rays. Testing of the single-cavity module continues in the presence of the fringe field produced by the "MuCool magnet". The MuCool magnet is composed of two superconducting coils wound on a single bobbin in a configuration closely similar to that of the MICE focus coils. The test of the single cavity module in the MTA will therefore allow the collaboration to understand how the cavities will perform in MICE and to develop operating procedures in advance of the installation of the cavities at RAL.

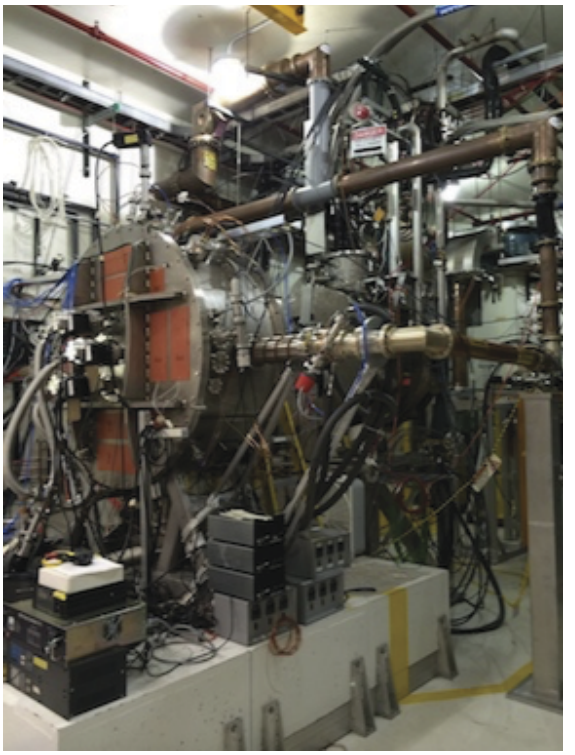


Figure 8: Photograph of the Single Cavity Test Stand installed in the Muon Test Area at Fermilab.

With the exception of the power couplers and tuner arms, all components of the second single-cavity module are available at Fermilab. Therefore, the principal tasks that must be completed to implement the MICE demonstration of ionization cooling are: the construction of the spool piece required to support the LiH absorber; the extension of the PRY to accommodate the

single cavity modules; and the rearrangement of the infrastructure in the MICE Hall to accommodate the new experimental arrangement. The collaboration is confident that this can be accomplished such that commissioning of the experiment in the new configuration can start in the late spring of 2017.

5. Conclusions

The MICE collaboration is now on track to deliver its demonstration of ionization cooling by 2017.

At Step IV, the properties of liquid hydrogen and lithium hydride that affect the performance of an ionization-cooling channel will be measured. The Step IV configuration will also be used to study the dependence of the ionization-cooling effect on the optics of the channel and the momentum and emittance of the input beam. Step IV construction is well advanced and commissioning will start in the spring of 2015.

The MICE demonstration of ionization cooling will be performed using a lithium-hydride absorber and with acceleration provided by two single, 201 MHz, cavity modules. Preparations for the MICE demonstration of ionization cooling are underway. The necessary equipment is either in hand (the superconducting magnets and instrumentation) or at an advanced stage of preparation (the single-cavity modules).

The demonstration of ionization cooling that MICE will provide is essential for the provision of the intense, well characterised muon beams required to elucidate the physics of flavour at the Neutrino Factory or to deliver multi-TeV lepton-antilepton collisions at the Neutrino Factory. The successful completion of the MICE programme will therefore herald the establishment of a new technique for particle physics.

Acknowledgements

I thank the organisers for the opportunity to present the work of the international Muon Ionizaation Cooling Experiment at the 2014 International Conference on High Energy Physics. I am indebted to my MICE colleagues for their hard work in developing the MICE programme, constructing the experiment and extracting the results.

[1] S. Choubey, R. Gandhi, S. Goswami, J. Berg, R. Fernow, et al., International Design Study for the Neutrino Factory, Interim Design Report.

[2] A. Bandyopadhyay, et al., Physics at a future Neutrino Factory and super-beam facility, Rept. Prog. Phys. 72 (2009) 106201. arXiv:0710.4947, doi:10.1088/0034-4885/72/10/106201.

[3] M. Apollonio, et al., Accelerator design concept for future neutrino facilities, JINST 4 (2009) P07001. arXiv:0802.4023, doi:10.1088/1748-0221/4/07/P07001.

[4] T. Abe, et al., Detectors and flux instrumentation for future neutrino facilities, JINST 4 (2009) T05001. arXiv:0712.4129, doi:10.1088/1748-0221/4/05/T05001.

[5] S. Ozaki, R. B. Palmer, M. S. Zisman, J. C. Gallardo, Feasibility Study-II of a Muon-Based Neutrino Source, Tech. Rep. BNL-52623, Brookhaven National Laboratory, Upton, NY (2001).

[6] Y. Kuno, et al., A feasibility study of a neutrino factory in japan, `http://www-prism.kek.jp/nufactj/` (May 2001).

[7] D. Finley, N. Holtkamp, A feasibility study of a neutrino source based on a muon storage ring, Nucl. Instrum. Meth. A472 (2000) 388–394.

[8] S. Geer, Neutrino beams from muon storage rings: Characteristics and physics potential, Phys. Rev. D57 (1998) 6989–6997. arXiv:hep-ph/9712290, doi:10.1103/PhysRevD.57.6989.

[9] D. M. Kaplan, A Staged Muon-Based Neutrino and Collider Physics ProgramarXiv:1212.4214.

[10] J. C. Gallardo, et al., Muon Collider: Feasibility Study, prepared for 1996 DPF / DPB Summer Study on New Directions for High Energy Physics (Snowmass 96), Snowmass, Colorado, 25 Jun - 12 Jul 1996 (1996).
URL `http://www.cap.bnl.gov/mumu/pubs/snowmass96/-part6.pdf`

[11] D. Neuffer, Principles and Applications of Muon Cooling, Conf.Proc. C830811 (1983) 481.

[12] K. Olive, et al., Review of Particle Physics, Chin.Phys. C38 (2014) 090001. doi:10.1088/1674-1137/38/9/090001.

[13] The MICE collaboration, MICE: An International Muon Ionization Cooling Experiment, MICE-0021 (2003).

[14] J. Wood, Scientific approval of mice, mICE Note 53 (2003).

[15] M. Bogomilov, et al., The MICE Muon Beam on ISIS and the beam-line instrumentation of the Muon Ionization Cooling Experiment, JINST 7 (2012) P05009. arXiv:1203.4089, doi:10.1088/1748-0221/7/05/P05009.

[16] D. Adans, et al., Characterisation of the muon beams for the Muon Ionisation Cooling Experiment, Submitted to JINSTarXiv:1306.1509.

[17] M. Ellis, et al., The design, construction and performance of the MICE scintillating fibre trackers, Nucl. Instrum. Meth. A659 (2011) 136–153. arXiv:1005.3491, doi:10.1016/j.nima.2011.04.041.

[18] M. Bogomilov, The MICE particle identification system, Nucl.Phys.Proc.Suppl. 215 (2011) 316–318. doi:10.1016/j.nuclphysbps.2011.04.042.

[19] R. Asfandiyarov, A totally active scintillator calorimeter for the Muon Ionization Cooling Experiment (MICE). Design and construction, Nucl.Instrum.Meth. A732 (2013) 451–456. doi:10.1016/j.nima.2013.08.026.

[20] G. Kafka, P. Snopok, J. Cobb, C. Rogers, Solid Absorber Program Status for MICE Step IV, Conf.Proc. C110904 (2011) 859–861.

[21] S. Ishimoto, S. Suzuki, M. Yoshida, M. Green, Y. Kuno, et al., Liquid Hydrogen Absorber for MICE, Conf.Proc. C100523 (2010) 421–423.

[22] M. Petroff, M. Stapelbroek, Photon-Counting Solid-State Photomultiplier, IEEE TRANSACTIONS ON NUCLEAR SCIENCE 36 (1, Part 1) (1989) 158–162.

[23] M. Petroff, M. Atac, High-Energy Particle Tracking using Scintillation Fibers and Solid-State Photomultipliers, IEEE TRANSACTIONS ON NUCLEAR SCIENCE 36 (1, Part 1) (1989) 163–164.

[24] V. M. Abazov, et al., The Upgraded DØ Detector, Nucl. Instrum. Meth. A565 (2006) 463–537. arXiv:physics/0507191,

doi:10.1016/j.nima.2006.05.248.
[25] P. Rubinov, AFEII design specifications, fermilab TM-2488-PPD.